AIAA 2005-1006

43rd AIAA Aerospace Sciences Meeting and Exhibit,
January 10-13, 2005, Reno, Nevada

AIAA 2005-1006

Aerodynamic Design of Turbine Blades Using an Adjoint Equation Method

Hsiao-Yuan Wu * , and Feng Liu †
Department of Mechanical and Aerospace Engineering
University of California, Irvine, CA 92697-3975
Her-Mann Tsai ‡
Temasek Laboratories
National University of Singapore
Kent Ridge Crescent, Singapore 119260

Aerodynamic design of turbine blades using an adjoint equation method is studied. Two design cases are tested. The first one is an inviscid design case for a VKI turbine stator, and the design objective is to minimize the entropy generation rate of the blade subject to a prescribed blade loading. The second case is a viscous design case for a standard configuration 4 turbine stator. The design objective is to minimize the entropy generation rate subject to a prescribed mass-averaged exit flow angle. The penalty function method is applied to deal with the constrained optimization problems. A resultant cost function is defined as a weighted sum of the original cost function and the deviation from the constraint. The formulations of the adjoint systems are derived for both cases based on the flow governing equations and the design objectives. Numerical programs are implemented to perform the optimization design. For the inviscid design case, the method is able to effectively reduce the entropy generation rate while the constraint is precisely satisfied. Reduction of shock wave strength is observed. For the viscous design case, results using the Baldwin-Lomax turbulence model and results using laminar flow solutions are presented. The program is effective for both transonic and subsonic conditions, which means the method is able to deal with frictional effects in addition to reducing shock wave strength.

Nomenclature

a	Speed of sound
$\mathbf{A}_i$	Jacobian matrices, $\mathbf{A}_i = \frac{\partial \mathbf{f}_i}{\partial \mathbf{w}}$
B	Boundaries of ξ domain
C	Penalty function
c_p	Constant pressure specific heat
D	The computational domain (ξ domain)
$\mathbf{f}_i$	inviscid flux
$\mathbf{f}_{vi}$	viscous flux
$\mathbf{G}$	Gradient for optimization

*Graduate Researcher, Student Member AIAA
†Professor, Associate Fellow AIAA
‡Principal Research Scientist, Member AIAA

I	Cost function
K_{ij}	Transformation functions between the physical domain the computational domain, $K_{ij} = \frac{\partial x_i}{\partial \xi_j}$
m_f	mass flow rate
M	Resultant cost function
n_i	Unit normal vector in the ξ domain, pointing outward from the flow field
N_i	Unit normal vector in the physical domain, pointing outward from the flow field
R	Gas constant
s	Entropy per unit mass
S_{gen}	Entropy generation rate
$\mathbf{w}$	Conservative flow variables, $\mathbf{w} = \{\rho,\ \rho u_1,\ \rho u_2,\ \rho u_3,\ \rho E\}^T$
x_i	Coordinates in the physical domain
$\tilde{\beta}$	Mass-averaged exit flow angle
Λ	Weight of the penalty function
ξ_i	Coordinates in the computational domain
$\mathbf{\Psi}$	Co-state variables, $\mathbf{\Psi} = \{\psi_1, \psi_2, \psi_3, \psi_4, \psi_5\}^T$

I. Introduction

Computational Fluid Dynamics plays a more and more important role in aerodynamic design as modern computer technologies develop rapidly. High-fidelity computational solutions offer useful information that had to be obtained from expensive wind tunnel experiments before. Nowadays computational methods are not only used as an analysis tool but also an optimization tool for aerodynamic design problems. Some optimization process that used to take experiences and trials now can be done automatically by computers.

A typical optimization program usually includes a flow solver and an optimizer. The flow solver is used to analyze the flow and to evaluate the performance of the design. The optimizer is to modify the design so that the performance will be improved. In order to do this, gradient information of the performance with respect to the design variables is needed. A most intuitive way to obtain the gradient is the finite-difference method. Each design variable is perturbed one at a time, and the flow field is solved for each perturbation in order to evaluate the performance. There have been many applications of this method on aerodynamic design. For example, Reuther et al. studied the optimization design of supersonic wing-body configurations using the Euler equations.[1] Hager et al. considered transonic airfoil optimization using the Navier-Stokes equations.[2] The computational cost of the gradient using the above method is proportional to the number of design variables. Therefore the use of this method is restricted to design problems with very few design variables.

However, it is desirable to use more design variables in order to search through a wider range of possible designs and to obtain better performances. In this case the finite-difference method is not practicable. An alternative way is the adjoint equation method. Gradient information can be obtained by solving once the flow governing equations and once the adjoint equations. The cost for solving the adjoint equations is approximately the same as the cost for solving the flow equations, and it is independent of the number of design variables. Jameson pioneered aerodynamic optimization using the adjoint equation method.[3,4] In the last few years there have been major progresses on aerodynamic optimization design using this method for airfoils, wings, and wing-body combinations. However, there have been relatively less efforts put on turbomachinery cascade design. The authors studied the adjoint equation method and applied it to some simplified design cases previously.[5,6] In this study further effort is made to apply the method to turbomachinery blade design.

Turbine blade design is a multi-disciplinary problem. Although in this study only the aerodynamic performances are considered, there are still many different aspects that need to be taken into account. Different cost functions are defined for different design objectives. A way to consider more than one design

objectives at the same time is to define a resultant cost function as a weighted sum of each individual cost function. This resultant cost function is minimized to obtain a compromised result. Constraints in design problems can be treated in the same way. The deviations from the constraints are viewed as cost functions (or penalty functions). By including them in the resultant cost function, we take into account all the constraints. Then the problem is treated as an unconstrained optimization problem.

The definition of design objectives and cost functions are discussed in the next section. The formulations of the adjoint equation method are derived based on the flow governing equations and the design objectives. Numerical programs are implemented to perform the optimization design. Results of an inviscid design case and a viscous design case are shown and discussed.

II. Design Objectives

In this study, two design cases are tested. The first one is an inviscid design case for a VKI turbine stator. The design objective is to minimize the entropy generation rate of the blade. There are other possible choices, for example, the entropy generation per unit mass of air, the uniformity of flow properties at the exit face, and etc. For now the cost function I is defined as the entropy generation rate S_{gen}. A constraint is applied, which is to maintain the blade loading L at a prescribed value L_0, and the penalty function C is defined as $|L - L_0|$. The blade loading is defined as the force acting on the blade in the vertical direction. Then the resultant cost function is defined as:

$$M = I + \Lambda C = S_{gen} + \Lambda |L - L_0|$$

in which Λ is the weight of the penalty function C. Figure 1 shows the configuration of the VKI turbine stator. The isentropic exit Mach number is 1.45 and the inflow direction is parallel to the x-axis. It is a 2-D configuration, but a 3-D mesh is made in order to test a 3-D optimization program.

The second case is a viscous design case for a standard configuration 4 turbine stator. Figure 2 shows the geometric configuration. In this case:

$$M = I + \Lambda C = S_{gen} + \Lambda |\tilde{\beta} - \tilde{\beta}_0|$$

where $\tilde{\beta}$ is the mass-averaged exit flow angle:

$$\tilde{\beta} = \frac{\int_{B_0} \rho u_j \beta N_j dA}{\int_{B_0} \rho u_j N_j dA}$$

B_O is the outlet boundary.β is defined as

$$\beta = tan^{-1} \frac{u_\theta}{u_x}$$

$$\theta = tan^{-1} \frac{z}{y}$$

$\tilde{\beta}_0$ is a prescribed value. For a multi-stage turbine, it is a complicated problem to consider all stages at the same time. It is desirable to simplify the problem by looking at one blade row at a time. In that case, some constraints need to be enforced on the interfaces in order to let the blade work consistently with its adjacent rows. That is why the mass-averaged exit flow angle is fixed in this case. It is also assumed that the inflow angle is fixed everywhere on the inlet face.

The coordinates of every mesh point on the blade surface are considered as the design variables. The numbers of design variables are very large for both of the design cases. Therefore the adjoint equation method is considered instead of the finite-difference method.

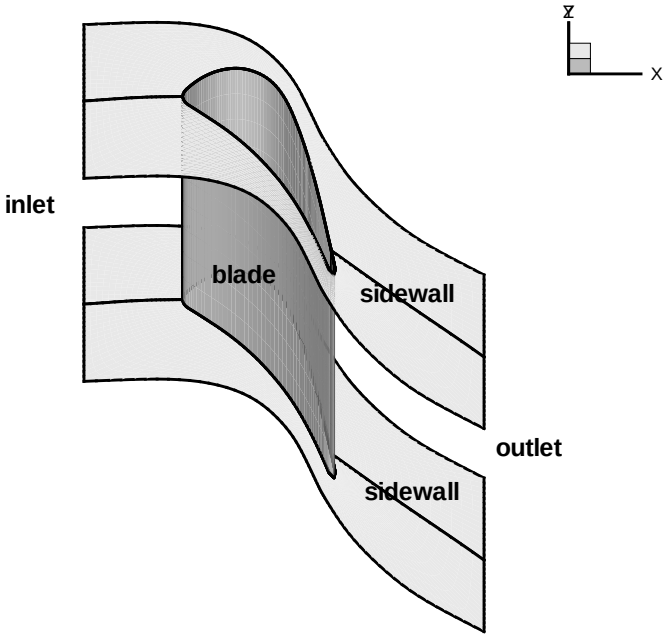

Figure 1. Configuration of the VKI turbine stator.

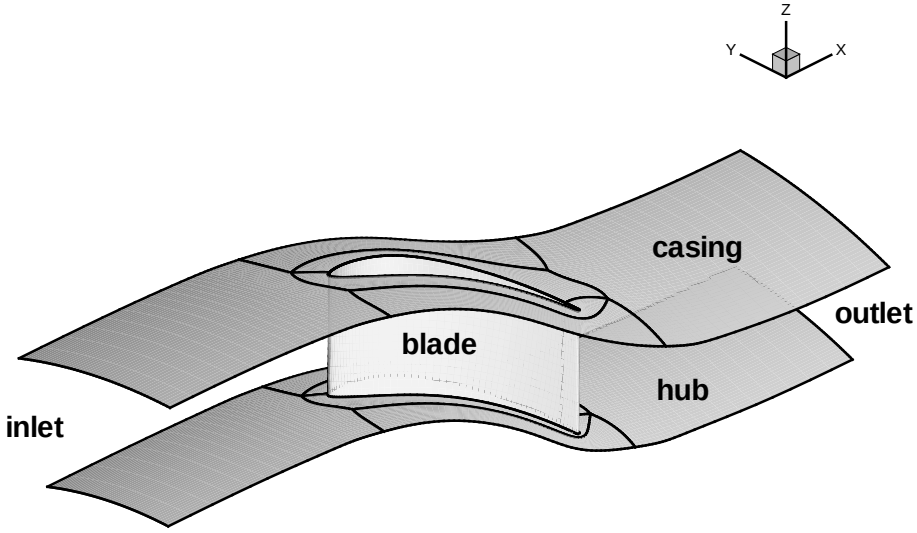

Figure 2. Configuration of the standard configuration 4 turbine stator.

III. Formulations of the Adjoint Equation Method

The derivation of the formulations follows that by Jameson.[7] The basic ideas are the same for both inviscid and viscous design cases. The following is an illustration of the derivation for the viscous design case. Only steady state conditions are considered in this study. The flow governing equations are the Reynolds Averaged Navier-Stokes equations. The Baldwin-Lomax turbulence model is adopted.

A weak form of the Navier-Stoke equations is

$$\int_B n_i \mathbf{\Psi}^T (\mathbf{F}_i - \mathbf{F}_{vi}) dB - \int_D \frac{\partial \mathbf{\Psi}^T}{\partial \xi_i} (\mathbf{F}_i - \mathbf{F}_{vi}) dD = 0$$

where $\mathbf{F}_i = S_{ij}\mathbf{f}_j$, $\mathbf{F}_{vi} = S_{ij}\mathbf{f}_{vj}$, $S_{ij} = JK^{-1}_{ij}$, $K_{ij} = \frac{\partial x_i}{\partial \xi_j}$, $, J = det(\{K_{ij}\})$, and

$$f_j = \begin{Bmatrix} \rho u_j \\ \rho u_1 u_j + \delta_{1j} p \\ \rho u_2 u_j + \delta_{2j} p \\ \rho u_3 u_j + \delta_{3j} p \\ \rho u_j H \end{Bmatrix}, \quad f_{vj} = \begin{Bmatrix} 0 \\ \sigma_{j1} \\ \sigma_{j2} \\ \sigma_{j3} \\ u_i \sigma_{ji} + k \frac{\partial T}{\partial x_j} \end{Bmatrix}$$

$$\sigma_{ij} = \mu(\frac{\partial u_i}{\partial x_j} + \frac{\partial u_j}{\partial x_i}) + \lambda \delta_{ij} \frac{\partial u_k}{\partial x_k}$$

$\mathbf{\Psi}$ is an arbitrary multiplier. If the blade shape and thus the flow field are perturbed, the equations for the variations are:

$$\int_B n_i \mathbf{\Psi}^T (\delta\mathbf{F}_i - \delta\mathbf{F}_{vi}) dB - \int_D \frac{\partial \mathbf{\Psi}^T}{\partial \xi_i} (\delta\mathbf{F}_i - \delta\mathbf{F}_{vi}) dD = 0$$

For turbulent flows, the total viscosity μ is a function of flow variables and the geometry, and it depends on the turbulence model implemented. However, in the derivation of the adjoint formulations, the variation $\delta\mu$ is assumed to be negligible during one design cycle. This is reported to be a reasonable approximation.[8]

For cases in which I, and C can be represented as boundary integrals, we have

$$\delta M = \delta I + \Lambda \delta C = \int_B (\delta Q_I + \Lambda \delta Q_C) dB$$

In this particular case

$$\delta Q_I = n_i \delta(\rho s u_j S_{ij}) \quad \text{on } B_O, \text{ and } \quad \delta Q_I = 0 \quad \text{on other boundaries.}$$

$$\delta Q_C = \frac{\Lambda^*}{\Lambda} \left[\frac{n_i}{m_f} \delta(\rho u_j \beta S_{ij}) - \frac{n_i \tilde{\beta}}{m_f} \delta(\rho u_j S_{ij}) \right] \quad \text{on } B_O, \text{ and } \quad \delta Q_C = 0 \quad \text{on other boundaries.}$$

where

$$\Lambda^* = \begin{cases} \Lambda & \text{if } \tilde{\beta} \geq \tilde{\beta}_0 \\ -\Lambda & \text{otherwise} \end{cases}$$

Adding the weak form of the Navier-Stokes equations to δM, we have:

$$\delta M = \int_B (\delta Q_I + \Lambda \delta Q_C) dB + \int_B n_i \mathbf{\Psi}^T (\delta\mathbf{F}_i - \delta\mathbf{F}_{vi}) dB - \int_D \frac{\partial \mathbf{\Psi}^T}{\partial \xi_i} (\delta\mathbf{F}_i - \delta\mathbf{F}_{vi}) dD$$

Next we want to separate geometric variation terms and flow variation terms. The geometric variation terms are kept, but flow variation terms need to be eliminated by properly assigning the values of the multiplier $\mathbf{\Psi}$. After some algebra:

$$
\begin{aligned}
\delta M \quad = \quad & \int_B \{ \quad \delta Q_I + \Lambda \delta Q_C - n_i \mathbf{\Psi}^T S_{ij} \mathbf{A}_j \delta \mathbf{w} \\
& \quad + n_i S_{ij} (\psi_{k+1} + \psi_5 u_k)(\delta \sigma_{jk}) + n_i S_{ij} \psi_5 \sigma_{jl} (\delta u_l) + n_i S_{ij} \psi_5 k \delta (\frac{\partial T}{\partial x_j}) \\
& \quad - \Gamma_{jk} n_k (\delta u_j) - (\delta T) S_{ij} \frac{\partial \psi_5}{\partial \xi_i} k \frac{\partial \xi_l}{\partial x_j} n_l \quad \} \quad dB \\
& + \int_D \{ \quad \frac{\partial \mathbf{\Psi}^T}{\partial \xi_i} S_{ij} \mathbf{A}_j (\delta \mathbf{w}) - [S_{il} \frac{\partial \psi_5}{\partial \xi_i} \sigma_{lj} - \frac{\partial}{\partial \xi_k} \Gamma_{jk}](\delta u_j) \\
& \quad + (\frac{\partial}{\partial \xi_l} [S_{ij} \frac{\partial \psi_5}{\partial \xi_i} k \frac{\partial \xi_l}{\partial x_j}])(\delta T) \quad \} \quad dD \\
& + \{\text{geometric variation terms}\} \qquad (1)
\end{aligned}
$$

Γ_{jk} is shown in the appendix.

For the domain integral of flow variations in Equation 1, collect the coefficients of $\delta w_1, \delta w_2, \delta w_3, \delta w_4$, and δw_5 . To eliminate explicit dependence of δM on $\delta \mathbf{w}$ in the domain, set the coefficients to zero, and then we obtain the adjoint equations.

Next consider the boundary integral of flow variations in Equation 1. Similar to the procedure shown above, we collect the coefficient of each independent flow variation, set the coefficients to zero, and then we obtain the boundary conditions for $\mathbf{\Psi}$. This way we can eliminate the explicit dependence of δM on flow variations on the boundaries. The adjoint equations and the boundary conditions are shown in the appendix.

When $\mathbf{\Psi}$ satisfies the adjoint equations and the boundary conditions, it is called the co-state variables. After the solutions of the flow equations and the adjoint equations are obtained, the gradient information can be obtained by evaluating the geometric variation integrals. No additional flow evaluation is needed.

IV. Numerical Methods

Although only steady state solutions are considered in this study, a time marching method is used to solve the flow equations and the adjoint equations. The properties of the adjoint equations are very similar to the flow equations, and many numerical schemes for flow solvers can be applied to the adjoint solvers as well. A finite volume method with artificial dissipation scheme (JST scheme) is used. The multi-grid method is used to accelerate the computation.

Structured meshes are made for both design cases. The meshes are divided into several blocks, and the program is parallelized to further accelerate the computation. Moreover, during the design process, the solutions of the previous flow evaluation or adjoint equation evaluation can be used as the initial conditions in order to reduce the number of iterations needed.

After the gradient information is obtained, an implicit smoothing scheme is applied to the gradient in order to maintain the smoothness of the blade surface. The conjugate gradients, instead of the gradients themselves, are used for optimization. a 1-D search scheme is implemented to accelerate the descent of the cost function.

V. Results

A. The Inviscid Design Case for the VKI Turbine Stator

Figure 3 shows the history of the normalized entropy generation rate and Figure 4 shows the corresponding normalized blade loading for different values of Λ. When Λ is large, the constraint for blade loading is strongly enforced, but the entropy generation rate does not decrease by much. Whereas when Λ is small,

the entropy generation rate decreases more, but the constraint for blade loading is not strictly satisfied. A proper value needs to be selected for a good design result. It depends on the actual design requirements. With $\Lambda = 0.1$, the deviation from the constraint is within the truncation error, and the entropy generation rate decreases by 14.5%. It shows the design method is effective. Since this is an inviscid design case, the

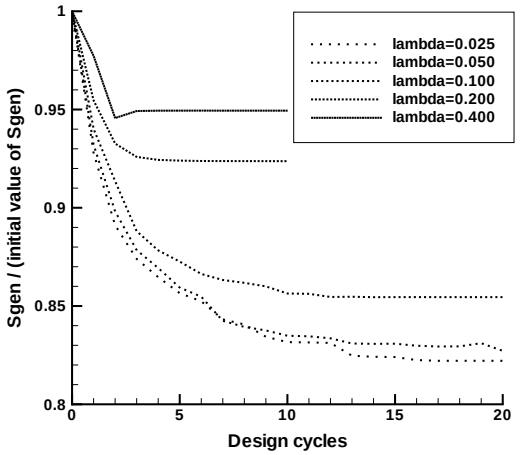

Figure 3. History of the entropy generation rate.

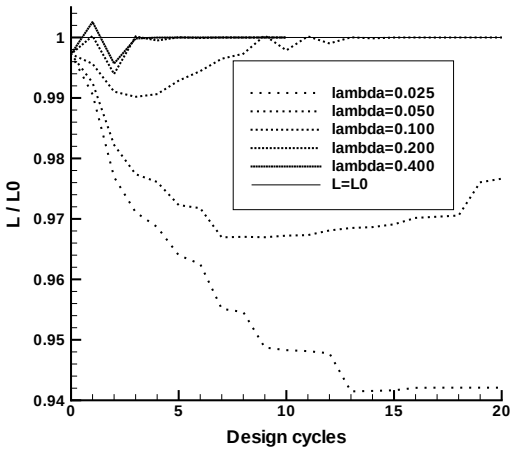

Figure 4. History of the blade loading.

entropy generation is due to the shock waves alone. (Ignore the effects of artificial dissipation.) Figure 5 shows the comparison of pressure contours between the initial blade and a designed blade. The designed blade has weaker shock waves around it, and that explains the reduction of entropy generation.

B. The Viscous Design Case for the Standard Configuration 4

Figure 6 shows the mesh for this design case. No-slip boundary condition is applied to the blade surface, but the hub and casing are assumed to be inviscid. This blade has a weak shock wave on the suction side near the root of the trailing edge under the designed operation condition. Reynolds number is about 2.5×10^6.

The maximal residuals of the flow solver go down for more than three orders with the current implementation of the Baldwin-Lomax turbulence model. However, It is observed that the value of S_{gen} is very sensitive to flow variable variations. Aftre the residuals reach their minimal levels, the fluctuation of S_{gen} due to time marching iterations is about the order of $\frac{1}{1000}$ of its mean value, while the fluctuation percentage of the mass flow rate of the passage is about one order smaller.

Currently only very limited results using the Baldwin-Lomax model are available. They are shown in Figures 7, 8, and 9. More systematic examinations of the program are being conducted. Figure 7 shows the history of the resultant cost function M, Figure 8 shows the corresponding history of the entropy generation rate S_{gen}, and Figure 9 shows the deviation from the constraint $(\tilde{\beta} - \tilde{\beta}_0)$. The values of M and S_{gen} are normalized by their initial values. $\tilde{\beta}_0 = 71.731^o$, and $\Lambda = 1000$. The fluctuation of S_{gen} may cause problems for the 1-D search scheme. In order to avoid this problem, a fixed step size for design modification is used currently. As we can see from the figures, although there are fluctuations, the trend of the data points is correct. The program is able to reduce M, S_{gen}, and maintain the magnitude of deviation from the constraint within a reasonable range.

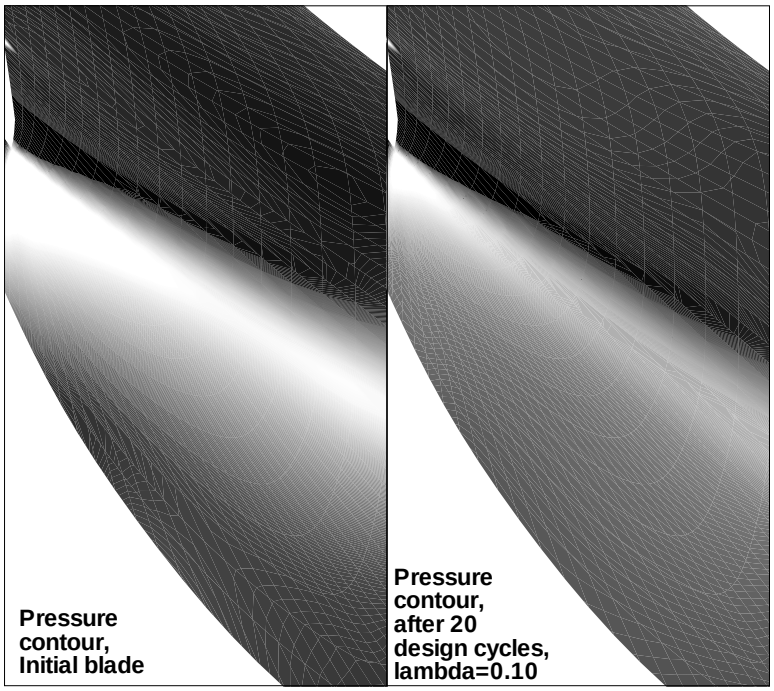

Figure 5. Comparison of pressure contours of shock waves.

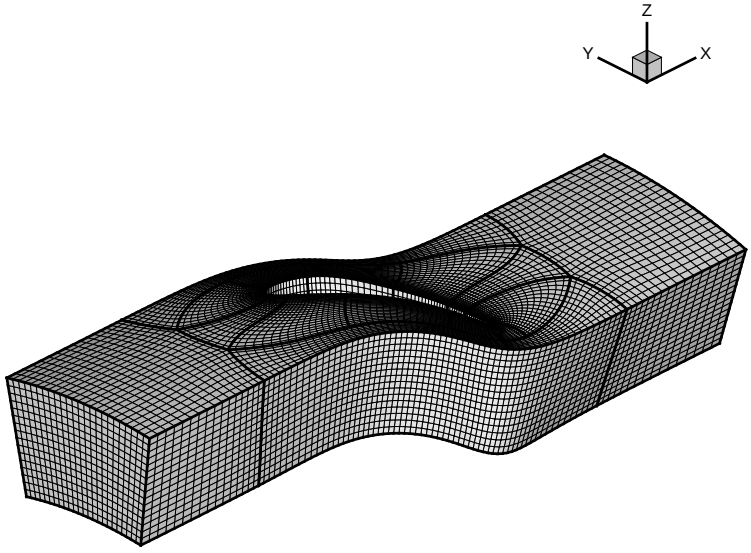

Figure 6. Mesh for the standard configuration 4 turbine stator.

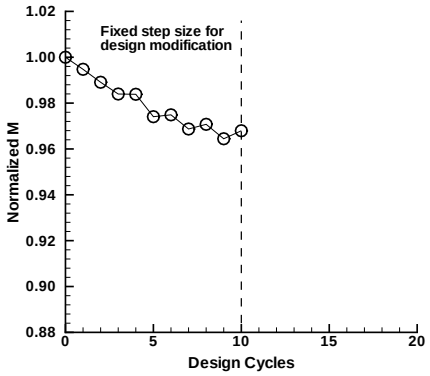

Figure 7. History of M, transonic case, with the Baldwin-Lomax model.

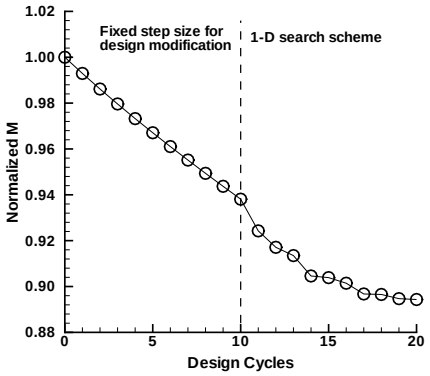

Figure 10. History of M, transonic case, with laminar flow solution.

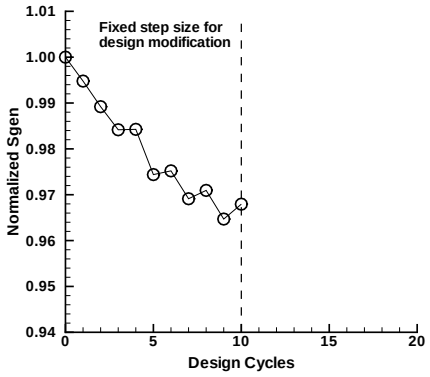

Figure 8. History of S_{gen}, transonic case, with the Baldwin-Lomax model.

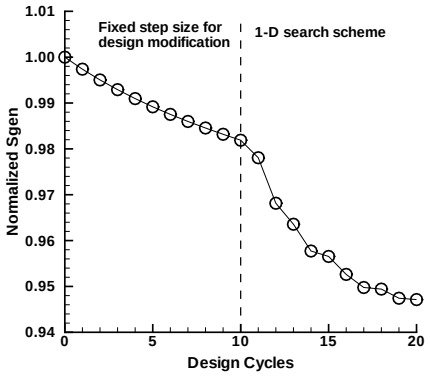

Figure 11. History of S_{gen}, transonic case, with laminar flow solution.

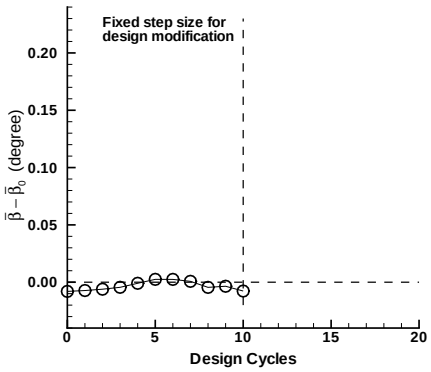

Figure 9. History of $(\tilde{\beta} - \tilde{\beta}_0)$, transonic case, with the Baldwin-Lomax model.

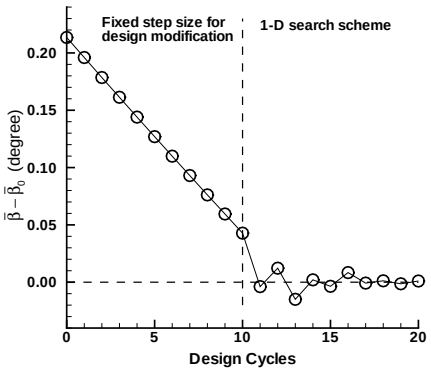

Figure 12. History of $(\tilde{\beta} - \tilde{\beta}_0)$, transonic case, with laminar flow solution.

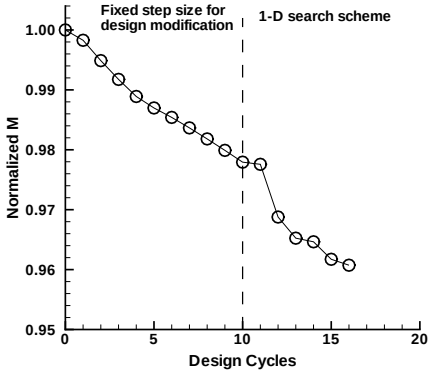

Figure 13. History of M, subsonic case, with laminar flow solutions.

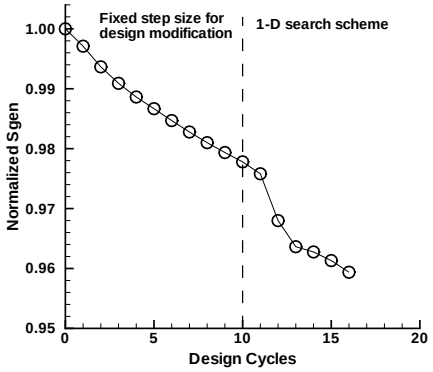

Figure 14. History of S_{gen}, subsonic case, with laminar flow solutions.

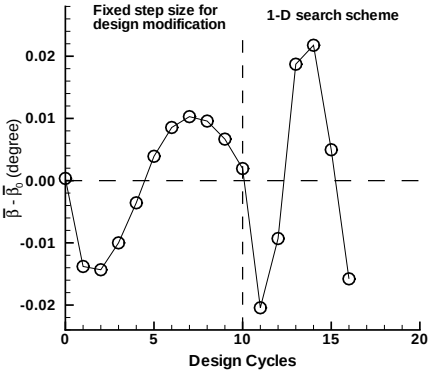

Figure 15. History of $(\tilde{\beta} - \tilde{\beta}_0)$, subsonic case, with laminar flow solutions.

The program was initially tested with laminar flow solutions and the results are also presented. Although they may not reflect the realistic flow conditions precisely, they help to validate the optimization method. Figures 10, 11, and 12 show the history of the normalized M, the normalized S_{gen}, and the deviation from the constraint, respectively. $\tilde{\beta}_0 = 71.620^o$, and $\Lambda = 4000$. A fixed step size for design modification is used for the first ten design cycles, and the 1-D search scheme is applied for the next ten design cycles. With a laminar flow solver, the fluctuation of S_{gen} due to time marching iteration is much smaller than the change due to optimization, and the 1-D search scheme works reasonably. With the total 20 design cycles, the resultant cost function δM is reduced by 11.6 % and the entropy generation rate S_{gen} is reduced by 5.3 %. The deviation from the specified exit flow angle drops from 0.196 degrees to 0.001 degrees. The results show that this optimization method is effective.

In order to see what the program can do on the frictional effects in addition to reducing the shock wave strength, a purely subsonic design case is tested. Laminar flow solutions are used. The back pressure is increased by 10% compared to the previous transonic case, and the maximal Mach number within the domain is about 0.93 in this case. $\tilde{\beta}_0 = 72.010^o$ and $\Lambda = 1000$. Results are shown in Figures 13, 14, and 15. The program is able to reduce the entropy generation rate by 4.1% in 16 cycles while keeping the deviation of the exit flow angle within ± 0.022 degrees. In this case $\tilde{\beta}_0$ is very close to the mass-averaged exit flow angle of the initial blade. During the design process, although the deviation from the constraint sometimes increases, the penalty function method maintains the magnitude of the deviation within a reasonable range. Results show that the optimization method is not only able to reduce the entropy generation due to shock waves, but also able to reduce the entropy generation due to frictional (viscous) effects.

VI. Conclusions

Two cases of turbine blade design using the adjoint equation method are studied. The first one is an inviscid design case for a VKI turbine stator. The objective is to minimize the entropy generation rate subject to a specified blade loading. The second case is a viscous design case for the standard configuration 4 turbine stator. The objective is to minimize the the entropy generation rate subject to a specified exit flow angle. The penalty function method is used to deal with the constrained optimization problems. For the inviscid design case, the program is able to achieve significant reduction of entropy generation while the loading constraint is precisely satisfied. An observation of pressure contours shows that the shock wave strength is reduced. For the viscous design case, the design results for turbulent flows and laminar

flows are presented. A transonic case and a subsonic case are tested. Results show that the optimization method is not only able to reduce the entropy generation due to shock waves, but also able to reduce entropy generation due to viscous effects.

Appendix

The adjoint formulations for the viscous design case:

A. The Adjoint Equations

$$\mathbf{A}_j^T \frac{\partial \mathbf{\Psi}}{\partial x_j} + \frac{1}{J}\tilde{\mathbf{M}}^{-1T}\tilde{\mathbf{V}} = 0$$

where

$$\tilde{\mathbf{V}} = \left\{ \begin{array}{c} -\frac{p}{R\rho^2}\frac{\partial}{\partial \xi_l}(k\frac{\partial \psi_5}{\partial \xi_i}\frac{\partial \xi_i}{\partial x_j}S_{lj}) \\ -\frac{\partial \psi_5}{\partial \xi_i}S_{il}\sigma_{l1} + \frac{\partial}{\partial \xi_m}\Gamma_{1m} \\ -\frac{\partial \psi_5}{\partial \xi_i}S_{il}\sigma_{l2} + \frac{\partial}{\partial \xi_m}\Gamma_{2m} \\ -\frac{\partial \psi_5}{\partial \xi_i}S_{il}\sigma_{l3} + \frac{\partial}{\partial \xi_m}\Gamma_{3m} \\ \frac{1}{R\rho}\frac{\partial}{\partial \xi_l}(k\frac{\partial \psi_5}{\partial \xi_i}\frac{\partial \xi_i}{\partial x_j}S_{lj}) \end{array} \right\}$$

$$\Gamma_{jk} = S_{ij}(\frac{\partial \psi_{l+1}}{\partial \xi_i} + \frac{\partial \psi_5}{\partial \xi_i}u_l)\mu\frac{S_{kl}}{J} + S_{il}(\frac{\partial \psi_{j+1}}{\partial \xi_i} + \frac{\partial \psi_5}{\partial \xi_i}u_j)\mu\frac{S_{kl}}{J} + S_{im}(\frac{\partial \psi_{l+1}}{\partial \xi_i} + \frac{\partial \psi_5}{\partial \xi_i}u_l)\lambda\delta_{lm}\frac{S_{kj}}{J}$$

$\tilde{\mathbf{M}}$ is defined as

$$\delta\mathbf{w} = \tilde{\mathbf{M}}\delta\tilde{\mathbf{w}}$$

where $\tilde{\mathbf{w}} = \{\rho,\ u_1,\ u_2,\ u_3,\ p\}^T$

B. Boundary Conditions

- On the inlet boundary B_I: ($s = 0$)

$$A^*_{i,j}P_j\psi_i = 0$$

where $A^*_{i,j}$ are components of $\mathbf{A}^*$, and

$$\mathbf{A}^* = n_i S_{ij}\mathbf{A}_j$$

$$\left\{ \begin{array}{c} P_1 \\ P_2 \\ P_3 \\ P_4 \\ P_5 \end{array} \right\} = \left\{ \begin{array}{c} 1 \\ \frac{u_1(u_iu_i - a^2)}{u_ju_j} \\ \frac{u_2(u_iu_i - a^2)}{u_ju_j} \\ \frac{u_3(u_iu_i - a^2)}{u_ju_j} \\ \frac{(1-\gamma)}{2}u_ju_j - a^2 + \gamma E \end{array} \right\}$$

- On the outlet boundary B_O: ($n_1 = -1,\ n_2 = 0,\ n_3 = 0$)

$$(A^*_{k,j+1} + A^*_{k,1}\tilde{K}_{j+1})\psi_k = \Lambda^*(\Theta_{j+1} + \tilde{K}_{j+1}\Theta_1) + \Pi_{j+1} + \tilde{K}_{j+1}\Pi_1, \quad j = 1,2,3$$

$$(A^*_{k,5} + A^*_{k,1}\tilde{K}_5)\psi_k = \Lambda^*\tilde{K}_5\Theta_1 + \tilde{K}_5\Pi_1$$

where

$$\tilde{K}_1 = 0,\ \ \tilde{K}_2 = \frac{2u_1}{u_ju_j},\ \ \tilde{K}_3 = \frac{2u_2}{u_ju_j},\ \ \tilde{K}_4 = \frac{2u_3}{u_ju_j},\ \ ,\tilde{K}_5 = -\frac{2}{u_ju_j}$$

$$\begin{Bmatrix} \Theta_1 \\ \Theta_2 \\ \Theta_3 \\ \Theta_4 \\ \Theta_5 \end{Bmatrix} = \begin{Bmatrix} -\frac{\rho u_j}{m_f} g_{bw1} S_{1j} \\ -\frac{\rho u_k}{m_f} S_{1k} g_{bw2} - \frac{\beta}{m_f} S_{11} + \frac{\tilde{\beta}}{m_f} S_{11} \\ -\frac{\rho u_k}{m_f} S_{1k} g_{bw3} - \frac{\beta}{m_f} S_{12} + \frac{\tilde{\beta}}{m_f} S_{12} \\ -\frac{\rho u_k}{m_f} S_{1k} g_{bw4} - \frac{\beta}{m_f} S_{13} + \frac{\tilde{\beta}}{m_f} S_{13} \\ 0 \end{Bmatrix}$$

$$\begin{Bmatrix} \Pi_1 \\ \Pi_2 \\ \Pi_3 \\ \Pi_4 \\ \Pi_5 \end{Bmatrix} = \begin{Bmatrix} u_j S_{1j} c_p \\ -s S_{11} \\ -s S_{12} \\ -s S_{13} \\ 0 \end{Bmatrix}$$

$$\begin{Bmatrix} g_{bw1} \\ g_{bw2} \\ g_{bw3} \\ g_{bw4} \\ g_{bw5} \end{Bmatrix} = \begin{Bmatrix} -\frac{1}{\rho}(u_1 \frac{-u_\theta}{u_x^2+u_\theta^2} + u_2 \frac{-u_x sin\theta}{u_x^2+u_\theta^2} + u_3 \frac{u_x cos\theta}{u_x^2+u_\theta^2}) \\ \frac{1}{\rho} \frac{-u_\theta}{u_x^2+u_\theta^2} \\ \frac{1}{\rho} \frac{-u_x sin\theta}{u_x^2+u_\theta^2} \\ \frac{1}{\rho} \frac{u_x cos\theta}{u_x^2+u_\theta^2} \\ 0 \end{Bmatrix}$$

- On the inviscid hub and casing surfaces B_X:

$$N_i \psi_{i+1} = 0$$

- On the viscous blade surface B_W:

$$\psi_2 = 0, \quad \psi_3 = 0, \quad \psi_4 = 0, \quad \frac{\partial \psi_5}{\partial N} = 0$$

- On the periodic boundary B_P: ψ_1,and ψ_5 are treated as scalars; (ψ_2, ψ_3, ψ_4) is treated as a vector.

C. Variation of the resultant cost function M in terms of geometric variations:

$$\delta M = \int_D \frac{\partial \mathbf{\Psi^T}}{\partial \xi_i} (\delta S_{ij})(\mathbf{f}_j - \mathbf{f}_{vj}) dD - \int_D S_{ij} \frac{\psi_5}{\partial \xi_i} k \frac{\partial T}{\partial \xi_l} \delta(\frac{\partial \xi_l}{\partial x_j}) dD - \int_D S_{ij} (\frac{\partial \psi_{l+1}}{\partial \xi_i} + \frac{\partial \psi_5}{\partial \xi_i} u_l)(\delta \sigma^*_{jl}) dD$$

where

$$\delta \sigma^*_{jl} = \mu[\delta(\frac{\partial \xi_l}{\partial x_j}) \frac{\partial u_k}{\partial \xi_l} + \delta(\frac{\partial \xi_l}{\partial x_k}) \frac{\partial u_j}{\partial \xi_l}] + \lambda \delta_{jk} \delta(\frac{\partial \xi_l}{\partial x_m}) \frac{\partial u_m}{\partial \xi_l}$$

References

[1] Reuther, J., Cliff, S., Hicks, R., and Van Dam, C., "Practical Design Optimization of Wing/Body Configurations Using the Euler Equations," AIAA Paper 92–2663, 1992.

[2] Hager, J., Eyi, S., and Lee, K., "Design Efficeincy Evaluation for Transonic Airfoil Optimization: A Case for Navier-Stokes Design," AIAA Paper 93–3112, AIAA 24th AIAA 24th Fluid Dynamics Conference, Orlando, Florida, July 1993.

[3] Jameson, A., "Aerodynamic Design via Control Theory," *Journal of Scientific Computing*, Vol. 3, 1988, pp. 233–260.

[4] Jameson, A., "Optimum Aerodynamic Design Using CFD and Control Theory," AIAA Paper 95–1729, AIAA 12th Computational Fluid Dynamics Conference, San Diego, California, june 1995.

[5] Yang, S., Wu, H., and Liu, F., "Aerodynamic Design of Cascades by Using an Adjoint Equation Method," AIAA Paper 2003-1068, AIAA 41st Aerospace Sciences Meeting and Exhibit, Reno, Nevada, January 2003.

[6]Wu, H. and Liu, F., "Comparison of Three Geometric Representations of Airfoils for Aerodynamic Optimization," AIAA Paper 2003-4095, AIAA 16th Computational Fluid Dynamics Conference, Orlando, Florida, June 2003.

[7]Jameson, A., "Aerodynamic Shape Optimization Using the Adjoint Method," Lectures at the von karman institute,brussels, Febuary 2003.

[8]Dreyer, J., "Hydrodynamic Shape Optimization of Propulsor Configurations Using a Continuous Adjoint Approach," Thesis, Department of Mechanical Engineering, Pennsylvania State University, May 2002.